



CHALMERS

Chalmers Publication Library

Low noise terahertz MgB₂ hot-electron bolometer mixers with an 11GHz bandwidth

This document has been downloaded from Chalmers Publication Library (CPL). It is the author's version of a work that was accepted for publication in:

Applied Physics Letters (ISSN: 0003-6951)

Citation for the published paper:

Novoselov, E. ; Cherednichenko, S. (2017) "Low noise terahertz MgB₂ hot-electron bolometer mixers with an 11GHz bandwidth". Applied Physics Letters, vol. 110(4),

Downloaded from: <http://publications.lib.chalmers.se/publication/246824>

Notice: Changes introduced as a result of publishing processes such as copy-editing and formatting may not be reflected in this document. For a definitive version of this work, please refer to the published source. Please note that access to the published version might require a subscription.

Chalmers Publication Library (CPL) offers the possibility of retrieving research publications produced at Chalmers University of Technology. It covers all types of publications: articles, dissertations, licentiate theses, masters theses, conference papers, reports etc. Since 2006 it is the official tool for Chalmers official publication statistics. To ensure that Chalmers research results are disseminated as widely as possible, an Open Access Policy has been adopted. The CPL service is administrated and maintained by Chalmers Library.

(article starts on next page)

Low noise terahertz MgB₂ hot-electron bolometer mixers with an 11GHz bandwidth

E. Novoselov^{a)} and S. Cherednichenko^{a,b)}

Terahertz and Millimetre Wave Laboratory, Department of Microtechnology and Nanoscience, Chalmers University of Technology, SE-412 96 Gothenburg, Sweden

Terahertz (THz) hot-electron bolometer mixers reach a unique combination of low noise, wide noise bandwidth, and high operation temperature when 6nm thick superconducting MgB₂ films are used. We obtained a noise bandwidth of 11GHz with a minimum receiver noise temperature of 930K with a 1.63THz Local Oscillator (LO) and a 5K operation temperature. At 15K and 20K, the noise temperature is 1100K and 1600K, respectively. From 0.69THz to 1.63THz the receiver noise increases by only 12%. Device current-voltage characteristics are identical when pumped with LOs from 0.69THz up to 2.56THz, and match well with IVs at elevated temperatures. Therefore, the effect of the THz waves on the mixer is totally thermal, due to absorption in the π conduction band of MgB₂.

THE MANUSCRIPT

Low noise terahertz (THz) heterodyne receivers are utilized to detect molecular emission lines from stars and interstellar medium, as well as for continuum observations, provided a large intermediate frequency (IF) bandwidth is available (several GHz). For frequencies of <1THz, Superconductor-Insulator-Superconductor (SIS) tunnel junction mixing provides sensitivity at a level of 2-5 photon energies. However, >1THz superconducting Hot-Electron Bolometer (HEB) mixers are the device of choice.¹ Although HEB mixers² are traditionally made of the same materials as SIS mixers, HEB mixers do not have any upper frequency operation limit and have been proven to work at least up to 5THz.³ Despite the apparent advantage over SIS, HEB mixers show excellent noise performance in a rather limited IF band: the 3dB noise bandwidth of NbN HEB mixers (currently, the most frequently used HEB mixers) is not more than 4-5GHz.^{4,5,6} The IF range >5GHz becomes unusable. The discussed limitation of NbN HEB mixers is determined by the limited HEB mixer gain bandwidth (GBW) caused by a finite electron energy relaxation rate.

Hot electrons in NbN films cool via two sequential processes: inelastic electron-phonon scattering ($\tau_{e-ph}=12ps$ at 10K,⁷ which is a typical critical temperature, T_c for thin NbN films) and phonon escape to the substrate ($\tau_{esc}(ps)=10\times d(nm)$,⁸ where d is the film thickness in nm). Critical temperature drops substantially in very thin films, thus setting a technological limit for the NbN HEB mixer.

^{a)} E. Novoselov and S. Cherednichenko contributed equally to this work.

^{b)} Electronic mail: serguei@chalmers.se

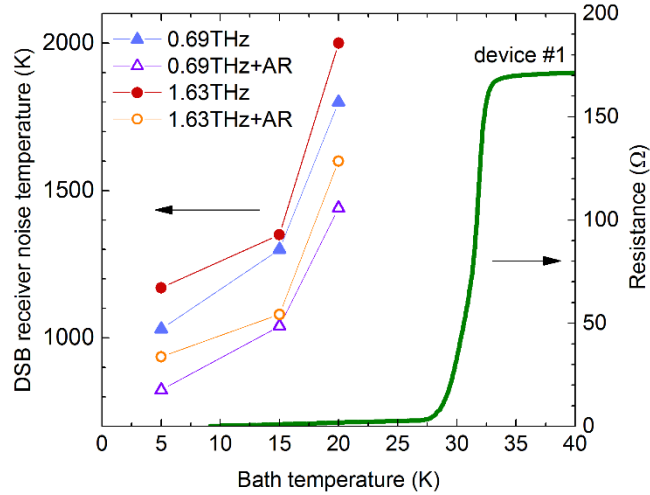


FIG. 1. Resistance versus temperature (R-T) curve for device #1 (line). Summary of the receiver noise temperature at 0.69THz (triangles) and 1.63 THz (circles). Empty symbols are for T_r corrected for the Si lens AR coating effect.

Since electron-phonon interaction time in MgB_2 was observed to be approximately 1-2ps,⁹ thin MgB_2 films were suggested for HEB mixers.¹⁰ With critical temperature, T_c of 39K in bulk films as thin as 20nm with a T_c of 20-22K have been fabricated using Molecular Beam Epitaxy (MBE).¹¹ Apart from a short electron-phonon interaction time, a very good acoustic match between MgB_2 films and substrates was observed, with a gain bandwidth of 2GHz for 20nm thick MgB_2 films.¹⁰ Although a Double Sideband (DSB) receiver noise temperature, T_r of 700K has been demonstrated at both 0.6THz¹² and 1.6THz,¹³ these devices were made of MgB_2 films with a T_c of 9K, and the noise bandwidth (NBW) (the IF where T_r rises x2 of its value at zero IF) did not exceed 3.5GHz. Using 20nm MgB_2 films with a T_c of 22K, T_r of 1700K was achieved with a NBW of 5GHz.¹³ Reduction of the film thickness below 20nm led to a drop of T_c . The next step forward was made with MgB_2 thin films deposited by Hybrid Physical Chemical Vapor Deposition (HPCVD) and 10-20nm thick films with a $T_c = 33\text{K}-37\text{K}$ have been obtained. This resulted in a GBW of 6-8GHz (compared to 2-3GHz for NbN HEB mixers).^{14,15} Further improvement in MgB_2 film deposition has been shown in Ref. 16. Initially thicker MgB_2 films (40nm) were thinned down to 2nm with a T_c of 28K. Yet no mixers have been fabricated of such films. In our paper we demonstrate MgB_2 HEB mixers made of very thin films (~6nm). These mixers combine a low noise temperature, wide IF bandwidth, and a high operation temperature.

For MgB_2 film deposition we utilized the HPCVD method.¹⁷ Our deposition system with the key parameter optimization has been presented in Ref. 18. The diborane (5% of B_2H_6 in H_2) and hydrogen flows were 2-5 sccm and 400 sccm, respectively, with a process pressure of 20 Torr. The substrate was SiC, with only a 0.42% lattice mismatch to the c-axis oriented MgB_2 . Film thickness was proportional to the deposition time, times the diborane flow, as has been verified using Transmission

In Applied Physics Letters, vol.110, n.4, 23 Jan. 2017.

Electron Microscopy (TEM) on 10nm and 20nm thick films, and using a profilometer and an atomic force microscope (AFM) for thicker films. At the discussed thicknesses the deposition rate is approximately 0.8-0.9Å/s for a diborane flow of 2sccm. For the deposition time of 70 s, the estimated film thickness is approximately 6nm. Unprocessed MgB₂ films had a T_c of 35-36K, a room temperature sheet resistance, R_s of 50Ω/sqr, and a residual resistance ratio (RRR) of 2.5 (tested with films on small witness substrates). Directly after MgB₂ film deposition the substrate was transferred (with a vacuum break) to a magnetron sputtering system, where, after a 10 minute Ar-ion cleaning, a 20nm Au layer was deposited. Preliminary tests showed that a cleaning process of 25 minutes increases the film sheet resistance (at room temperature) by 5-10%. This cleaning step appears to be vital for achieving low noise temperature at THz frequencies.

HEB mixers are essentially microbridges from 0.3μm×0.3μm to 1μm×1μm size, integrated with a logarithmic spiral antenna. The antenna is made of a 250nm thick gold film. The 20nm gold layer on top of the microbridge is removed using an ion-milling process. The exposed MgB₂ film is protected with a thin SiN_x layer. The critical temperature of the devices was 30K (see Figure1 for the R-T curve of device#1, however similar R-T curves have been measured for all samples of the batch). The critical current density at 4.2K was $(1.2-2.0) \times 10^7 \text{A/cm}^2$ (see Figure 2). Although such a high J_c indicates thin MgB₂ films of high quality, some scattering of the critical currents and normal state resistances probably points to some variations of film defects/thickness across the substrate. Published morphology studies of 5-10nm thick MgB₂ films, also made with HPCVD, showed¹⁷ that MgB₂ films were not fully connected, and that there were gaps of tens of nanometers between islands of MgB₂ for films thinner than 15nm. We have not yet been able to conduct morphology studies on our films; however, it appears that in our case, MgB₂ films merge into a continuous structure at smaller thicknesses than previously reported. This could be caused by a significantly lower deposition rate in our system, compared to e.g. (3Å/s)¹⁹. As the result we were able to fabricate submicron size devices with $T_c > 30\text{K}$ from films thinner than 10nm.

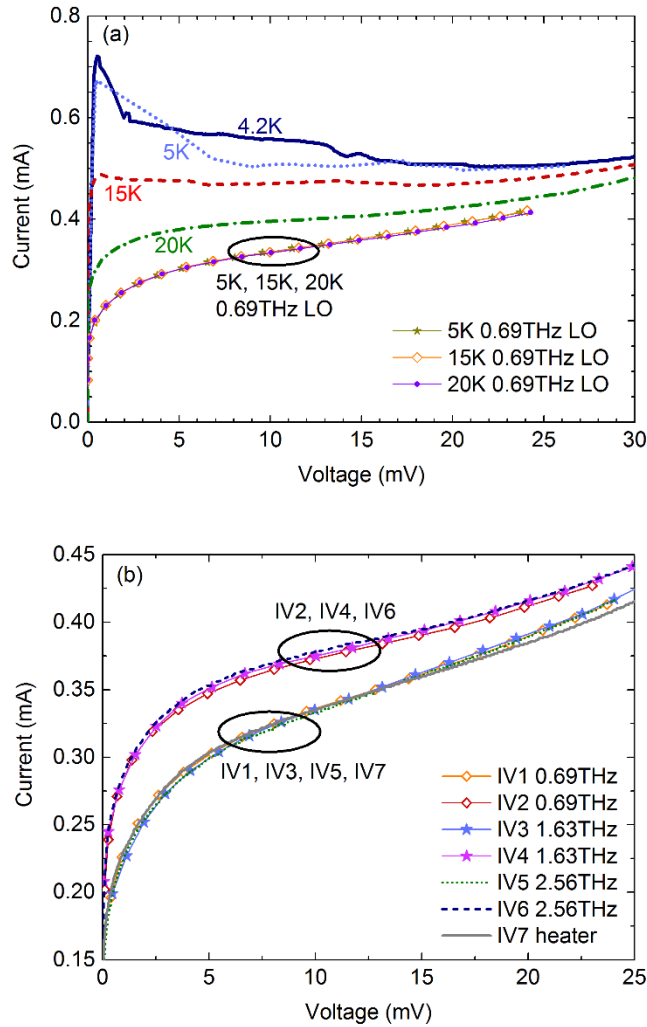


FIG. 2 (a) The mixer IV-curves (light blue dotted) without LO pumping at 4.2K (in the dip-stick), in the cryostat at 5K (no LO, blue solid), at 15K (no LO, red dashed), at 20K (no LO, green dash-dotted). Three (fully overlapping) IVs at the optimal LO power at 5K, 15K; and 20K. (b) two sets of IVs at different LO power levels, all at 5K: under the 0.69THz, 1.63THz, and 2.56THz LO pumping. No difference between curves pumped with the mentioned LOs can be observed. IV7 (grey solid) is recorded for the HEB at an elevated temperature without LO pumping.

Two $1\mu\text{m}\times 1\mu\text{m}$ size mixers were tested at THz frequencies. These had room temperature resistances of 205Ω and 230Ω . Current-voltage (IV) characteristics for device #1 are given in Figure 2. For device #2, the $I_c(4.2\text{K})$ was 0.97mA , with very similar IVs (under THz radiation), noise temperature and the bandwidth as for device #1. Therefore, further discussion will concern only device #1. R_S obtained from the micro bridges appears to be a factor of 4 higher than for the unprocessed films (see above). The increase of R_S is in line with a reduction of T_c by 4K. More study is needed to find out whether both effects originate in the device fabrication procedure, or are due to micro defects in the original films, which appear on the micrometer scale. 15-20nm thick MgB_2 films did not show significant variation of film properties before or after device fabrication.

TABLE I. Optical loss included in the receiver noise temperature measurements: the 50cm air path, the cryostat window, and the infrared filters. Calibration for Si lens reflection loss is used only in Fig.1.

Frequency	Air path	Window	IR filters	Si Reflection ^a
0.69THz	0.03dB	0.7dB	0.6dB	1dB
1.63THz	0.55dB	0.7dB	0.6dB	1dB

^a Reduction of the Si lens reflection from 1dB to 0.2dB can be achieved by application of Parylene C antireflection coating.²¹

In order to measure HEB mixer sensitivity at THz frequencies, the chip with the antenna integrated HEB was attached to the back (flat) side of a 5mm elliptical Si lens (without an antireflection coating,²⁰ which could reduce the optical loss by 0.8dB²¹). Apart from the Si lens and the chip, the mixer block contained a transition to an SMA connector and a heater. In front of the mixer block the beam was collimated with an off-axis parabolic aluminum mirror, also mounted in the cryostat. The actual HEB temperature was obtained from a comparison of the critical current, I_c in the mixer block with that obtained in the dip-stick. The IF chain consisted of a bias-T and a cryogenic Low Noise Amplifier (LNA) at 4.2K, two more LNAs, a tunable band pass YIG filter (50MHz bandwidth) and a microwave power meter at room temperature. Two sets of LNAs were used with bandwidths of 1.5-4.5GHz and 1-9GHz (the noise temperature is ~3-5K). A Far Infrared (FIR) gas laser was used as the local oscillator, with radiation emission frequencies of 0.69THz, 1.63THz, and 2.56THz. At 2.56THz the output power was not sufficient to pump the mixer with a thin beam splitter and hence, it was only used with a mirror to record IV-curves. Continuously chopped (1Hz) emissions from 295K/77K black body loads were used to measure the DSB receiver noise temperature as per Y-factor technique. It comprises the mixer noise temperature, the contributions from the IF chain and the input optics loss. A 12.5 μ m thick Mylar beam splitter combined the LO and the black body loads into the cryostat. Optical losses included in receiver noise temperature calculations from the Y-factor are given in Table I. The spiral antenna polarization is elliptical, and therefore exact knowledge of the polarization ellipse is required in order to calculate the transmission loss through the beam splitter. Consequently, beam splitter loss was neglected. Although a broadband spiral antenna was used, the direct detection effect²² was not observable presumably due to a larger LO power requirement of the discussed mixers. Furthermore, because the output noise versus the bias current (for a fixed voltage) is positive, a possible (though very small) direct detection effect does not lead to an overestimation of the Y-factor.

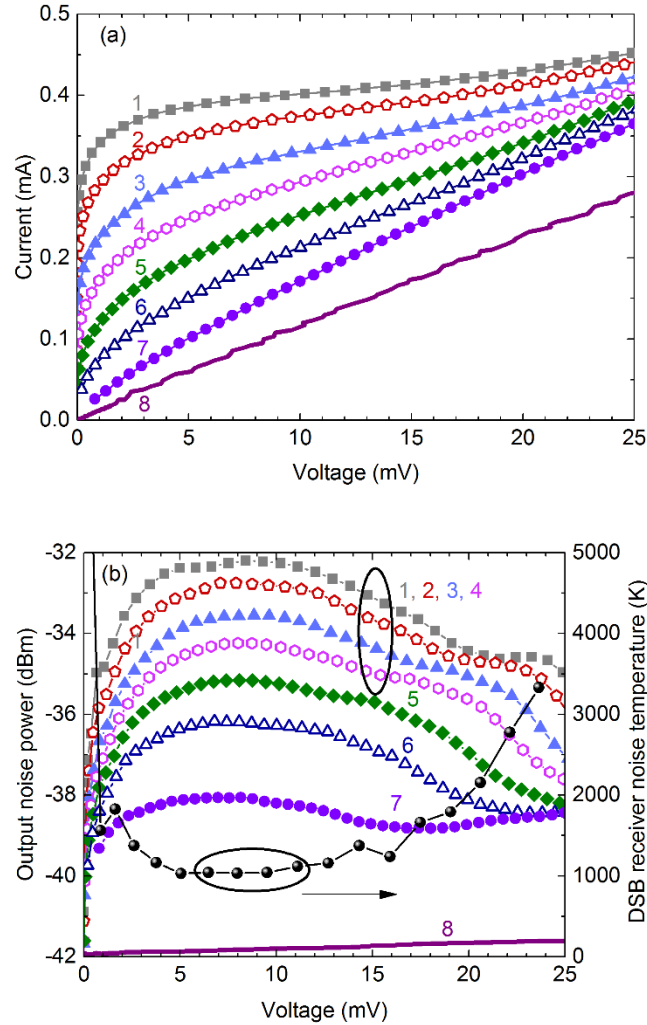


FIG. 3. (a) The mixer IV-curves at 5K under the 0.69THz LO pumping (curves 1-7), and without LO in the normal state ($\approx 35\text{K}$) (curve 8). (b) The output power (IF=2GHz) versus voltage curves corresponding to the IVs in (a). IV-curves 3-5 correspond to the lowest T_r (optimal LO power). The receiver noise temperature versus voltage curve corresponds to IV-curve 3.

Critical current, I_c of the mixer was measured in the dipstick to be 0.72mA at 4.2K, whereas I_c was 0.67mA in the cryostat (5K). IV curves of the mixer at 4.2K (dip-stick), and in the cryostat at different temperatures (without LO pumping) are given in Figure 2(a). With optimal LO (0.69THz) power the IVs at 5K, 15K, and 20K fully overlap each other, indicating that in the HEB the LO power at 0.69THz is absorbed independently of the temperature and the bias voltage. At 5K, the shape of the IVs was also observed not to depend on the LO frequency from 0.69THz to 2.56THz (Figure 2(b)). By switching off the LO and increasing the HEB temperature, IVs can be found to fully match IVs under the LO. In MgB_2 films with a T_c of $\sim 30\text{K}$ (similar to those discussed here) superconducting energy gaps, $\Delta(0)$ of 2.2meV and 5meV have been reported for π - and σ - conduction bands, respectively.²³ With optical gaps of 2Δ , the THz photon absorption should therefore occur in the π - band (see also

In Applied Physics Letters, vol.110, n.4, 23 Jan. 2017.

Ref.24), where $2\Delta/h \approx 1\text{THz}$, and thus explain the IVs in Figure 2(a) (h is the Planck constant). Laser output power was higher at 0.69THz, therefore most of the experimental data were obtained at this LO frequency. A set of IVs during LO pumping is given in Figure 3(a). The corresponding receiver output noise curves (all under the 295K load) and the optimal noise temperature curve are given in Figure 3(b). The shapes of the curves correspond with those of low- T_c HEB mixers, e.g. made of NbN.²⁵ Being also supported by other facts (no effect of LO frequency on IVs, a weak LO frequency dependence of T_r (see below)) we may conclude that the mixing response has a bolometric nature. The minimum on the T_r -V curve was found in the 5-10mV bias voltage range.

A summary of the measured T_r at both 0.69THz and 1.63THz LO frequencies at mixer temperatures of 5K, 15K, and 20K is given in Figure 1. Considering a reduction of the reflection loss at the Si lens by 20% when an AR coating is used,²¹ the minimum noise temperatures at 5K amount to 830K (0.69THz) and 930K (1.63THz). At 15K, T_r rises by 20% from its value at 5K. At 20K, T_r rises by 75%. As can be noticed, the noise temperature difference between 0.69THz and 1.63THz is about 12%. A similar rate of T_r increase vs LO frequency has been observed for NbN HEB mixers for LOs >1THz.²⁶

Detailed study of mixer conversion gain and noise versus operation temperature, and due comparison with the theory is beyond the scope of this paper. However, it is interesting to discuss some of the data provided by Figures 3(a),(b). In order to acquire intrinsic mixer parameters, a U-factor technique with a HEB in normal state (as a reference state) can be utilized.¹³ With the HEB at 5K and at minimum noise temperature point the U-factor is $\sim 8.5\text{dB}$ (Figure 3(b), curves 3 and 7), which gives a T_{out} of $\sim 210\text{K}$. An output noise of 40K-50K has been reported for NbN HEB mixers with a T_c of 9K.²⁶ At optimal bias point, T_{out} for HEB mixers is expected to be affected by two contributions: the temperature fluctuations noise ($\propto T_c^2$), and the Johnson noise ($\propto T_c$). Therefore, the obtained output noise temperature for MgB₂ mixers falls into the expected range. With both the receiver noise temperature and the output noise at hand, we can estimate the mixer gain to be approximately -9dB (the optical loss is not included in this figure).

The T_{out} of 210K is higher than the previously reported 80K for devices made of MgB₂ film with a T_c of 22K.¹³ We explain this fact by the higher T_c (30K vs 22K) used in the current work (see discussion above). The increased mixer gain from -15dB (from Ref. 13) to -9dB (this work) can be attributed to the same increase of the T_c (leading to a higher LO power, and hence to the mixer gain²⁷), as well as to the reduced antenna/HEB contact resistance achieved with in-situ cleaning. High mixer gain and high output noise is a preferred combination for heterodyne receivers, because it reduces the effect of the LNA noise in the IF readout.

Perhaps, the most interesting data presented here is the IF spectrum of the receiver noise temperature. Previously, a 3dB GBW of 6-8GHz had been reported for devices made of 10-15nm thick MgB₂ films.^{14,15} It has also been proven that GBW scales up inversely with film thickness.¹⁵ In our work, T_r was measured across a wide IF range using the afore mentioned two sets of LNAs. The data obtained with the 1-9GHz LNA and the 1.63THz LO are given in Figure 4. The data obtained with the 1.5-4.5GHz LNA (measurements were performed for redundancy) totally repeats these curves, including the hump at 3.7GHz, which is probably due to the mixer block or the bias-T. The fitting curve is for the noise bandwidth of 10.7GHz. No bias point effect on the NBW has been observed within the optimal bias range.

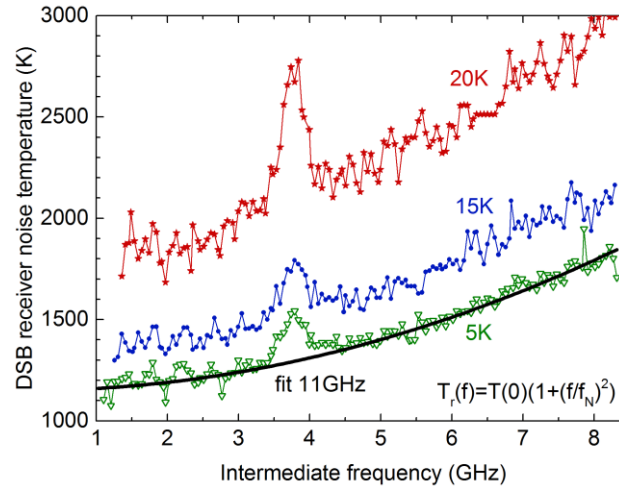


FIG. 4. The receiver noise (at 1.63 THz LO) as a function of the IF recorded at 5K, 15K, and 20K operation temperatures.

In summary, we demonstrated that a combination of low noise temperature ($\sim 1000\text{K}$) and wide noise bandwidth ($\sim 11\text{GHz}$) can be achieved with superconducting MgB₂ HEB mixers. Current devices were made from MgB₂ films as thin as $\sim 6\text{nm}$ with a T_c of $\sim 30\text{K}$. The small thickness provided the short phonon escape time from the film into the substrate, whereas the high T_c resulted in the short electron-phonon interaction time (which is inversely proportional to the electron temperature at the optimal operation point, $\approx T_c$). A weak dependence of T_r on LO frequency makes us optimistic in regard to the operation of current (or similar) devices at even higher frequencies (the goal is 5THz).

This work was financially supported by the European Research Council (ERC). The authors wish to thank Prof. X. X. Xi and Prof. K. Chen of Temple University for valuable discussions on MgB₂ films technology; and personnel of the Nanofabrication Laboratory (Chalmers University of Technology) for technical support.

REFERENCES

-
- ¹ H.-W. Hübers, IEEE J. Sel. Top. Quant. **14**, 378–391 (2008).
- ² E. M. Gershenzon, G. N. Gol'tsman, I. G. Gogidze, Y. P. Gusev, A. I. Elant'ev, B. S. Karasik, and A. D. Semenov, Sov. Phys. Supercond. **3**, 1582 (1990).
- ³ W. Zhang, P. Khosropanah, J. R. Gao, T. Bansal, T. M. Klapwijk, W. Miao, and S. C. Shi, J. Appl. Phys. **108** (9), 093102 (2010).
- ⁴ S. Cherednichenko, V. Drakinskiy, T. Berg, P. Khosropanah, and E. Kollberg, Rev. Sci. Instrum. **79**, 034501 (2008).
- ⁵ W. Zhang, W. Miao, J. Q. Zhong, S. C. Schi, D. J. Hayton, N. Vercruyssen, J. R. Gao, and G.N. Gol'tsman, Supercond. Sci. Technol. **27**, 085013 (2014).
- ⁶ C. Risacher, R. Güsten, J. Stutzki, H.-W. Hübers, D. Büchel, U. U. Graf, S. Heyminck, C. E. Honingh, K. Jacobs, B. Klein, T. Klein, C. Leinz, P. Pütz, N. Reyes, O. Ricken, H.-J. Wunsch, P. Fusco, and S. Rosner, IEEE Trans. THz Sci. Technol. **6**, 199–211 (2016).
- ⁷ K. S. Il'in, M. Lindgren, M. Currie, A. D. Semenov, G. N. Gol'tsman, R. Sobolevski, S. I. Cherednichenko, and E. M. Gershenzon, Appl. Phys. Lett. **76**, 2752 (2000).
- ⁸ S. Cherednichenko, P. Yagoubov, K. Il'in, G. Gol'tsman and E. Gershenzon, in *Proceedings of 27th European Microwave Conference*, Jerusalem, Israel, September 8-12 1997, pp. 972–977.
- ⁹ Y. Xu, M. Khafizov, L. Satrapiskiy, P. Kuš, A. Plecenik, and R. Sobolewski, Phys. Rev. Lett. **91**, 197004 (2003).
- ¹⁰ S. Cherednichenko, V. Drakinskiy, K. Ueda, and M. Naito, Appl. Phys. Lett. **90**, 023507 (2007).
- ¹¹ H. Shibata, T. Akazaki, and Y. Tokura, Supercond. Sci. Technol. **26**, 035005 (2013).
- ¹² S. Bevilacqua, E. Novoselov, S. Cherednichenko, H. Shibata, and Y. Tokura, IEEE Trans. Appl. Supercond. **25**, 2301104 (2015).
- ¹³ E. Novoselov, S. Bevilacqua, S. Cherednichenko, H. Shibata, and Y. Tokura, IEEE Trans. THz Sci. Technol. **6**, 238–244 (2016).
- ¹⁴ D. Cunnane, J. H. Kawamura, M. A. Wolak, N. Acharya, T. Tan, X. X. Xi, and B. S. Karasik, IEEE Trans. Appl. Supercond. **25**, 2300206 (2015).
- ¹⁵ E. Novoselov, N. Zhang, and S. Cherednichenko, Proc. SPIE **9914**, 99141N (2016).
- ¹⁶ N. Acharya, M. A. Wolak, T. Tan, N. Lee, A. C. Lang, M. Taheri, D. Cunnane, B. S. Karasik, and X. X. Xi, APL Mater. **4**, 086114 (2016).
- ¹⁷ X. X. Xi, A. V. Pogrebnyakov, S. Y. Xu, K. Chen, Y. Cui, E. C. Maertz, C. G. Zhuang, Q. Li, D. R. Lamborn, J. M. Redwing, Z. K. Liu, A. Soukiassian, D. G. Schlom, X. J. Weng, E. C. Dickey, Y. B. Chen, W. Tian, X. Q. Pan, S. A. Cybart, and R.C. Dynes, Phys. C, Supercond. **456**, 22–37 (2007).
- ¹⁸ E. Novoselov, N. Zhang, and S. Cherednichenko, “Study of MgB₂ ultra-thin films in submicron size bridges,” accepted for publication in IEEE Trans. Appl. Supercond. (December 2016).
- ¹⁹ M. A. Wolak, N. Acharya, T. Tan, D. Cunnane, B.S. Karasik, and X. X. Xi, IEEE Trans. Appl. Supercond. **25**, 7500905 (2015).
- ²⁰ A. J. Gatesman, J. Waldman, M. Ji, C. Musante, and S. Yngvesson, IEEE Microw. Guided Wave Lett. **10**, 264–266 (2000).
- ²¹ M. Kroug, S. Cherednichenko, H. Merkel, E. Kollberg, B. Voronov, G. Gol'tsman, H.-W. Hübers, and H. Richter, IEEE Trans. Appl. Supercond. **11**, 962 (2001).
- ²² S. Cherednichenko, V. Drakinskiy, T. Berg, E. L. Kollberg, and I. Angelov, IEEE Trans. Microw. Theory Techn. **55**, 504–510 (2007).
- ²³ M. Putti, M. Affronte, C. Ferdeghini, P. Manfrinetti, C. Tarantini, and E. Lehmann, Phys. Rev. Lett. **96**, 077003 (2006).
- ²⁴ M. Ortolani, P. Dore, D. Di Castro, A. Perucchi, S. Lupi, V. Ferrando, M. Putti, I. Pallecchi, C. Ferdeghini, and X.X. Xi, Phys. Rev. B. **77**, 100507R (2008).
- ²⁵ J. Kawamura, R. Blundell, C. E. Tong, G. Gol'tsman, E. Gershenzon, B. Voronov, and S. Cherednichenko, Appl. Phys. Lett. **70**, 1619 (1997).
- ²⁶ W. Zhang, P. Khosropanah, J.R. Gao, E.L. Kollberg, K.S. Yngvesson, T. Bansal, R. Barends, and T.M. Klapwijk, Appl. Phys. Lett. **96**, 111113 (2010).
- ²⁷ B. S. Karasik and A. I. Elant'ev, Appl. Phys. Lett. **68**, 853 (1996).